

Determination of the spin diffusion length in germanium by spin optical orientation and electrical spin injection

C Rinaldi^{1,2}, S Bertoli¹, M Asa¹, L Baldrati¹, C Manzoni³, M Marangoni³, G Cerullo³, M Bianchi⁴, R Sordan⁴, R Bertacco^{1,2} and M Cantoni¹

¹ Department of Physics, Politecnico di Milano, via G. Colombo 81, 20133 Milano, Italy

² IFN-CNR, Institute of Photonics and Nanotechnologies, piazza Leonardo da Vinci 32, 20133 Milano, Italy

³ Department of Physics, Politecnico di Milano, piazza Leonardo da Vinci 32, 20133 Milano, Italy

⁴ Department of Physics—L-NESS Center, Politecnico di Milano, via F. Anzani 42, 22100 Como, Italy

E-mail: matteo.cantoni@polimi.it

Received 21 April 2016, revised 7 July 2016

Accepted for publication 18 August 2016

Published 22 September 2016



CrossMark

Abstract

The measurement of the spin diffusion length and/or lifetime in semiconductors is a key issue for the realisation of spintronic devices, exploiting the spin degree of freedom of carriers for storing and manipulating information. In this paper, we address such parameters in germanium (001) at room temperature (RT) by three different measurement methods. Exploiting optical spin orientation in the semiconductor and spin filtering across an insulating MgO barrier, the dependence of the resistivity on the spin of photo-excited carriers in Fe/MgO/Ge spin photodiodes (spin-PDs) was electrically detected. A spin diffusion length of $0.9 \pm 0.2 \mu\text{m}$ was obtained by fitting the photon energy dependence of the spin signal by a mathematical model. Electrical techniques, comprising non-local four-terminal and Hanle measurements performed on CoFeB/MgO/Ge lateral devices, led to spin diffusion lengths of $1.3 \pm 0.2 \mu\text{m}$ and $1.3 \pm 0.08 \mu\text{m}$, respectively. Despite minor differences due to experimental details, the order of magnitude of the spin diffusion length is the same for the three techniques. Although standard electrical methods are the most employed in semiconductor spintronics for spin diffusion length measurements, here we demonstrate optical spin orientation as a viable alternative for the determination of the spin diffusion length in semiconductors allowing for optical spin orientation.

Keywords: germanium, polarimetry, photodetector, spin diffusion, optoelectronics

(Some figures may appear in colour only in the online journal)

1. Introduction

Semiconductor spintronics is a rapidly evolving field, aiming at employing the spin of electrons in semiconductor devices in order to extend existing electronic devices performances and, in a more perspective vision, to address new functionalities within the quantum domain, ranging from storage to computation [1]. A key parameter that determines performances and feasibility of semiconductor-based spintronic devices is the spin diffusion length in semiconductors (or, equivalently,

the spin lifetime). Many techniques, exploiting different spin-dependent physical mechanisms, from all-optical [2, 3], to all-electrical [4, 5], to hybrid methods (e.g. using radio-frequency [6] or ferromagnetic resonance [7]), have been employed for their measurement. A strict comparison between different methods on the same semiconductor template is lacking.

In this framework, Germanium spintronics has gained greater importance, due to the good spin transport and manipulation properties of Germanium and the integrability on Si-based structures through SiGe technology. The spin

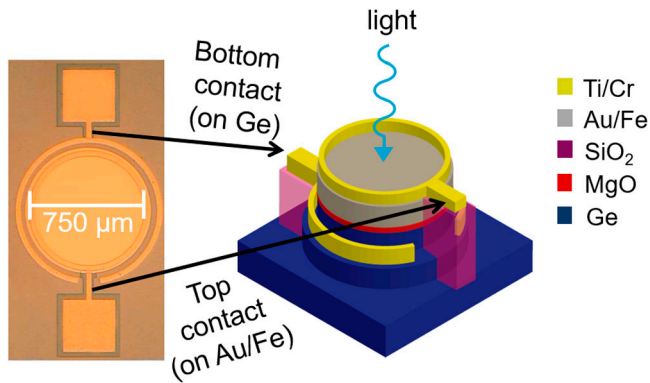


Figure 1. Top view picture (left) and 3D sketch (right) of a spin-photodiode.

lifetime in Ge is large enough to allow for spin transport over micrometric distances [8], while its large spin–orbit coupling permits spin manipulation [9].

Aiming at satisfying two of the key issues in semiconductor spintronics, i.e. the injection and the detection of spin polarized carriers in the semiconductor (SC), the Fe/MgO/SC template attracted a large interest [8, 10, 11]: it allows to solve the conductivity mismatch problem [12] and, thanks to the high spin selectivity at MgO/FM interface, where FM is a ferromagnetic materials such as Fe, Co and FeCoB [13], to obtain high spin filtering performances. The suitability of the Fe/MgO template with Ge(001) has largely been demonstrated [14–18], while the effective spin filtering across MgO in the Fe/MgO/Ge structure has been addressed both experimentally and theoretically in [11].

Between the different techniques exploiting the coupling between spin polarization and electrical transport in semiconductor spintronics devices, in the last few years spin-optoelectronics has emerged as a novel research area, unifying the spin-electronics and opto-electronics competences. Spin photodiodes (spin-PDs) based on Germanium have been successfully realized employing the Ni/Ge/AlGaAs structure by Shen *et al* [8], and subsequently employing the Fe/MgO/Ge template by some of the authors [11, 19]. These devices convert (i) the helicity of the impinging light into spin polarization of photo-excited carriers, thanks to the optical selection rules at the Γ point of the semiconductor bandstructure, and (ii) the spin polarization of photo-excited carriers into the modulation of the device resistance, thanks to the spin-dependent tunnelling across the MgO barrier in the Fe/MgO/Ge structure and the Schottky barrier in the Ni/Ge/AlGaAs structure. While these devices are typically intended as integrated polarimeters, scalable down to micro- or nano-metric dimensions, in this paper we show how they can be successfully employed as probing tools in order to measure the spin diffusion length in the semiconductor.

In section 3 we demonstrate that the ratio between the spin diffusion length and the light attenuation length in the semiconductor determines the factor of merit of the spin photodiode [11, 20, 21] in discriminating different helicity states. The behaviour of the factor of merit as a function of the photon energy allows the spin diffusion length in the semiconductor to be found by employing the simple mathematical model presented in section 3. In section 4 we use standard

electrical measurements [10], i.e. non-local (NL) transport measurements (section 4.1) and Hanle effect (section 4.2), to determine the spin diffusion length in independent ways, in order to confirm the results obtained by optical spin orientation. Our results finally demonstrate that the latter, based on the optical spin orientation versus photon energy and its detection by spin filtering across the Fe/MgO/Ge structure, is suitable for the determination of the spin diffusion length and provides results compatible with those obtained by more standard electrical methods.

2. Experiment

Spin-PDs based on the Au/Fe/MgO/Ge heterostructures were prepared by molecular beam epitaxy (MBE) in a customized ultra-high vacuum system [22]. We employed accidentally n-doped Ge(001) commercial wafers (resistivity $\rho \sim 47 \Omega \cdot \text{cm}$) in order to maximize the spin diffusion length. MgO and Fe were deposited on Ge at room temperature (RT) and post-annealed at 770 K and 470 K, respectively, to achieve good epitaxy with limited interdiffusion at the interfaces. The MgO and Fe thickness were fixed at 1.8 nm and 10 nm, respectively. Finally, the samples were capped with 2 nm of Au in order to protect the topmost Fe layer from oxidation. More details on the sample growth and characterization can be found in [16, 17]. Spin-PDs with circular shape and different areas (from 1×10^4 to $5 \times 10^5 \mu\text{m}^2$) were fabricated by means of optical lithography, ion beam etching and e-beam deposition. The resulting structure of devices is shown in figure 1.

The electrical measurements were performed both in NL geometry [10] and by Hanle and inverted Hanle effects (HE, IHE) [23]. These techniques represent standard validated tools for the determination of the spin diffusion length and the spin lifetime in semiconductors. A Ta(20 nm)/Co₄₀Fe₄₀B₂₀(10 nm)/MgO(2.5 nm) template was grown on Ge(001) by magnetron sputtering in an AJA Orion8 system, operating at a base pressure of about 1×10^{-9} mbar. The Ge(001) substrate was the same used for photodiodes. Prior to deposition, the Ge substrate was soft-etched *in situ* by Ar-ions plasma to remove the native oxide and annealed to 500 °C to restore the crystallographic order. The MgO layer was deposited in radio frequency mode, while the Ta and Co₄₀Fe₄₀B₂₀ (CoFeB) layers were deposited in dc mode. Annealing at 770 K and 470 K were performed after MgO and CoFeB deposition, respectively. Subsequently, an array of devices with suitable geometry was fabricated by the combined use of electron-beam and optical lithography, ion milling and e-beam deposition. Note that, unlike the case of spin-PDs, magnetron sputtering was employed instead of MBE and Ta/CoFeB was used instead of Au/Fe. These choices were driven by the following reasons: (i) to demonstrate that the MgO/Ge-based spin filter can be realized by magnetron sputtering as well, paving the way to a possible industrial implementation of such class of devices; (ii) to confirm that the measured quantities (spin diffusion length and lifetime) are mainly related to the details of the buried semiconductor (according to that, efficient spin filtering with MgO barrier can be achieved with both Au/Fe and Ta/CoFeB

overlayers). Minor differences could come from the choice of the ferromagnet [24], due to the different spurious magnetic moments arising from interface roughness (as explained in details below).

3. Spin optical orientation

Optical measurements were performed with the laser beam impinging on the photodiode perpendicularly to the top surface (Au/Fe side), as schematically show in figure 1. Left (σ^-) or right (σ^+) circularly polarized light crosses the Au, Fe and MgO layers and is finally absorbed in Ge, exciting spin polarized photo-carriers (electrons in the conduction band, holes in the valence band), according to the optical selection rules valid around the Γ point of the material band structure [25]. A voltage bias is applied between the two Au/Ti circular electrodes, contacting the Au/Fe (top contact) and Ge (bottom contact) sides of the spin-PD. A positive (negative) bias voltage drives photo-excited electrons (holes) from Ge to Au/Fe and thus produces an electrical photo-induced current. Thanks to the spin-dependent transmission across the Fe/MgO interface, the total resistance of the device depends on the relative orientation between the Fe magnetization (saturated out-of-plane by an external magnetic field collinear to the photon angular momentum) and the spin of carriers: the measurement of such a resistance allows to identify the carrier spin polarization (parallel/antiparallel to the external field) and, consequently, the light circular polarization (σ^- or σ^+). Previously [11, 26] we reported the first demonstration of the room temperature operation of a spin-PD based on the fully epitaxial Fe/MgO/Ge(001) heterostructure, operating in a wide wavelength range, from visible (400nm) to near infrared (1550nm), with the possibility to discriminate the two opposite circular light polarizations by a variation of the photo-induced current up to several percent. In this paper, we employ the wavelength dependence of the spin-photodiode response, at positive bias ($V_{\text{bias}} = 0.4\text{V}$), in order to find the spin diffusion length of electrons in Germanium.

In this regime, electrons photo-generated in Ge move towards the MgO barrier, preserving their spin if they are excited close to it with respect to the spin diffusion length l_s . We define ΔJ as the difference between the current densities flowing along the device when it is illuminated by right (σ^+) and left (σ^-) circularly polarized light ($\Delta J = J^{\sigma^+} - J^{\sigma^-}$), with a constant V_{bias} applied between the two contacts. ΔJ can be phenomenologically written as [11]

$$\Delta J = 2J_{\text{photo}}(D + A_{\text{SF}}) \quad (1)$$

J_{photo} is the photo-induced current generated upon illumination by linearly polarized light and with in-plane magnetization of Fe; D is the magnetic circular dichroism asymmetry related to the dichroic absorption of light by the Fe layer [11, 26]; A_{SF} is the spin-dependent transport asymmetry, which is the relevant quantity for understanding the spin transport properties of Ge. ΔJ depends on V_{bias} through the photo-induced current J_{photo} ; anyway, since we are working at constant V_{bias} , this dependence can be neglected in our analysis and the spin-dependent transport is enclosed in the term A_{SF} .

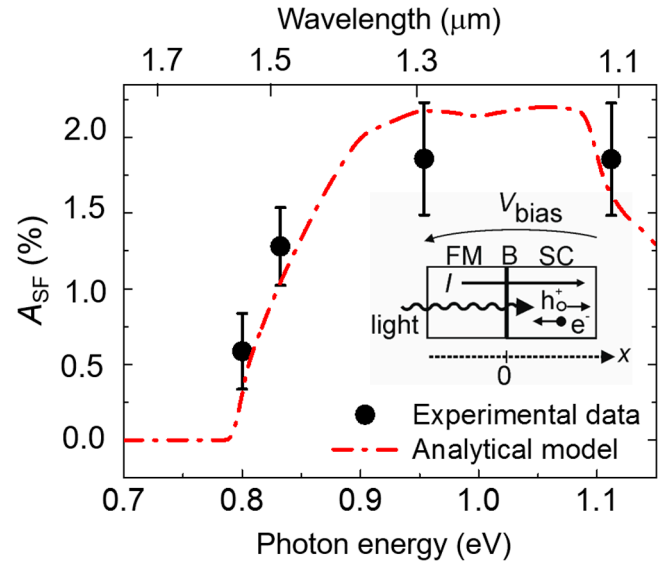


Figure 2. Experimental spin transport asymmetry A_{SF} (dots) and fitting with equation (8) (red line) versus photon energy [21]. A spin diffusion length $l_s = 0.9 \pm 0.2 \mu\text{m}$ can be extracted from the fit. In the inset, a basic scheme of the device, with the coordinate system used in the text, is reported. Reproduced with permission from [21]. Copyright 2014 SPIE.

The value of the spin transport asymmetry A_{SF} [11] depends on the photon energy $h\nu$ because of its relation with (i) the spin polarization of photo-excited carriers immediately after photo-generation (P_S as calculated in [25]) and (ii) the light attenuation length in Ge (λ_{Ge}) that determines the spatial distribution of spins within the semiconductor [27]. In order to extract the spin diffusion length (l_s), we developed a simple model for optical spin orientation and transport in Ge, which contains all relevant quantities as a function of the photon energy. The dichroic absorption of Fe is neglected because this contribution can be measured and easily subtracted from experimental data (being simply proportional to the total photocurrent I_{photo} through a coefficient D known from literature and experiments [11]).

The basic scheme of the device is reported in the inset of figure 2. When Ge, that we assume to be semi-infinite, is illuminated by light with a given helicity, the spin polarization immediately after the photo-generation is:

$$P_S = \frac{\eta^+ - \eta^-}{\eta^+ + \eta^-} \quad (2)$$

η^+ (η^-) is the photo-generation efficiency for carriers with spin parallel (antiparallel) to the light helicity. In the investigated region, $|P_S|$ varies smoothly from 0.5 at 0.8 eV (that is resonant with the direct bandgap at the Γ point of the Ge band structure) to 0.4 at 1.1 eV [25].

Light suffers an exponential attenuation due to absorption in Ge:

$$\begin{aligned} dn_{\text{ph}}(x) &= \frac{n_{\text{ph}}(0)}{\lambda_{\text{Ge}}} \exp(-x/\lambda_{\text{Ge}}) dx \\ &= \frac{1}{\lambda_{\text{Ge}}} \frac{E_{\text{light}}(0)}{h\nu} \exp(-x/\lambda_{\text{Ge}}) dx \end{aligned} \quad (3)$$

$n_{\text{ph}}(x)$ is the number of photons per unit area and time ($\text{m}^{-2} \text{s}^{-1}$) crossing a section of Ge at distance x from the MgO/Ge

interface; $n_{\text{ph}}(0)$ is the number of incoming photons per unit area and time at the MgO/Ge interface ($x = 0$); $dn_{\text{ph}}(x)$ is the number of photons per unit area and time absorbed in Ge between x and $x + dx$; $E_{\text{light}}(0)$ is the irradiance (W m^{-2}) at the MgO/Ge interface ($x = 0$); λ_{Ge} is the light attenuation length at the photon energy $h\nu$. At distance x from the interface, light creates electron-holes pairs, with spin parallel (+) and anti-parallel (−) to the light helicity:

$$dJ_{\text{photo}}^{+(-)}(x) = e\eta^{+(-)}dn_{\text{ph}}(x) = \eta^{+(-)}\frac{e}{\lambda_{\text{Ge}}}\frac{E_{\text{light}}(0)}{h\nu}\exp(-x/\lambda_{\text{Ge}})dx \quad (4)$$

$dJ_{\text{photo}}^{+(-)}(x)$ is the current density of +(-) photoelectrons generated by light absorption between x and $x + dx$; e is the electron charge.

The corresponding photo-induced current density asymmetry $d\Delta J_{\text{barrier}}$, defined as the difference between the current densities of + and − photoelectrons generated between x and $x + dx$ ($d\Delta J_{\text{photo}} = dJ_{\text{photo}}^+ - dJ_{\text{photo}}^-$) and arriving at the barrier with its spin polarization preserved, is

$$d\Delta J_{\text{barrier}}(x) = d\Delta J_{\text{photo}}(x)\exp(-x/l_s)f(V) = \Delta\eta\frac{e}{\lambda_{\text{Ge}}}\frac{E_{\text{light}}(0)}{h\nu}\exp(-x/\lambda_{\text{Ge}})\exp(-x/l_s)f(V)dx \quad (5)$$

where $\Delta\eta = \eta^+ - \eta^-$ and $f(V)$ takes into account the effect of the applied voltage (V_{bias}).

The total photo-induced current density asymmetry at the barrier can be calculated by integrating equation (5) over the Ge thickness, that we assume to be infinite (strictly, it is sufficient that it is much larger than the light attenuation length)⁵:

$$\Delta J_{\text{barrier}} = \int_0^\infty \Delta\eta\frac{e}{\lambda_{\text{Ge}}}\frac{E_{\text{light}}(0)}{h\nu}\exp(-x/\lambda_{\text{Ge}})\exp(-x/l_s)f(V)dx = \Delta\eta f(V)\frac{l_s}{\lambda_{\text{Ge}} + l_s}J^* \quad (6)$$

where we define $J^* = eE_{\text{light}}(0)/h\nu$.

The total current density of photoelectrons generated by linearly polarized light can instead be calculated as the integral of equation (4) over the Ge depth considering an equal number of spin-up and spin-down electrons:

$$J_{\text{photo}} = \int_0^\infty \frac{(\eta^+ + \eta^-)}{2}f(V)\frac{e}{\lambda_{\text{Ge}}}\frac{E_{\text{light}}(0)}{h\nu}\exp(-x/\lambda_{\text{Ge}})dx = \frac{(\eta^+ + \eta^-)}{2}f(V)J^* \quad (7)$$

Finally, the spin dependent transport asymmetry at the MgO/Ge interface can be found from equation (1) neglecting the dichroic term, as

$$A_{\text{SF}} = \frac{\Delta J_{\text{barrier}}}{2 \cdot J_{\text{photo}}} = P_S \frac{l_s}{\lambda_{\text{Ge}} + l_s} \quad (8)$$

In figure 2 we reported the experimental values of A_{SF} as a function of photon energy from 0.8 eV (1550 nm) to 1.10 eV (1130 nm). These energies are close to (or in coincidence with) the direct gap of Ge around the Γ point ($E_{\text{gap}} = 0.8$ eV), meaning that the photo-excited electrons possess very small energy above the local conduction band minimum (CBM) at Γ . After photo-generation, electrons relax with a very short characteristic time ($\tau_{\Gamma \rightarrow L} \sim 230$ fs [29]) from Γ to the absolute CBM at the L point of Ge, responsible for the electrical transport. This means that, despite the different mechanisms for spin injection (optical or electrical) discussed in this paper, all electrical transport processes deal with electrons lying at the CBM at the L point. Moreover, spin depolarization during the transition from Γ to L can be assumed to play a minor role, so that even the spin transport processes rely on the electrons lying at the bottom of the conduction band. These create the basic motivation to allow us to compare electrical and optical results.

From the fit (red continuous line) of A_{SF} extracted by experimental data (black dots) in figure 2, we finally obtained a spin diffusion length $l_s = 0.9 \pm 0.2 \mu\text{m}$, coherent with our previous reports [11]. Using $l_s = \sqrt{D\tau_s}$ and assuming a diffusion constant $D = 0.01035 \text{ m}^2 \text{ s}^{-1}$ for intrinsic Ge, the corresponding value of spin lifetime is $\tau_s \approx 80 \pm 40 \text{ ps}$ ⁶.

4. Electrical spin injection

4.1. Non-local spin transport

The experimental configuration for the NL measurements is shown in figure 3(a). Four-terminal devices were fabricated by the combined use of electron beam and optical lithography and the resulting structure is shown in figure 3(b). Terminals $T1$ and $T4$ are square pads with $50 \mu\text{m}$ side, while $T2$ and $T3$ are stripes of $2 \mu\text{m} \times 50 \mu\text{m}$ and $1 \mu\text{m} \times 50 \mu\text{m}$, respectively.

Inner terminals ($T2$ and $T3$) are separated by a distance in the order of the expected spin diffusion length, ranging from 0.6 to 2.4 μm in different devices. The outer terminals ($T1$ and $T4$) are located far away from the inner ones (namely 100 μm from $T2$ and $T3$, respectively). An in-plane variable magnetic field (H) is applied during the measurements by means of an external electromagnet, as in figure 3(a). The inner electrodes have two different coercive fields along the stripe because of their different shape anisotropy [30]. The in-plane relative orientation (parallel/antiparallel) of the magnetization of the inner electrodes can thus be controlled by the external magnetic field.

In four-terminal devices, spins injected in the semiconductor by $T2$ diffuse and generate a non-zero spin polarization

⁵ Note that, for simplicity, we neglected any band bending effect at the MgO/Ge interface. This approximation works quite well for spin-PDs based on MgO barriers, because of Fermi level depinning at the interface between MgO and Ge (see Lu *et al* [28]).

⁶ Note that the electron diffusion coefficient D was calculated by the Einstein relation from tabulated electron mobility data (see www.ioffe.ru/SVA/NSM/Semicond/Ge). The corresponding error on D is 5%. The error bars reported in the text include both the D contribution and the experimental errors on the measured quantities, l_{sf} or τ_s .

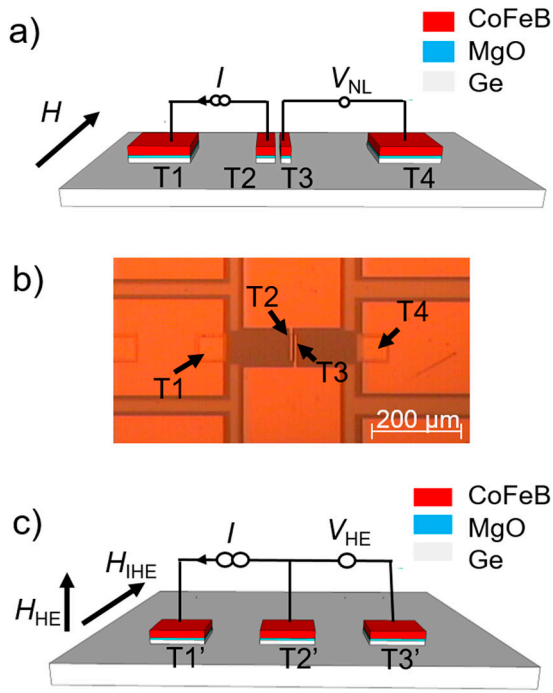


Figure 3. (a) Sketch of the device and setup for non-local measurements. (b) Top view of a non-local four-terminal device; (c) sketch of device and setup for Hanle and inverted Hanle effects.

in the surrounding region. Providing that the distance (d) between $T2$ and $T3$ is not too large with respect to the electron spin diffusion length (l_s), this non-zero spin polarization results in the splitting of the electrochemical potentials associated to the two spin channels at $T3$ [31], and in turns affects the non-local voltage (V_{NL}), measured between $T3$ and $T4$, related to the energy difference between the electrochemical potentials of the spin polarized terminal ($T3$) and the reference terminal ($T4$). The NL signal is finally defined as the ratio between the non-local voltage V_{NL} and the current I flowing between $T1$ and $T2$. From [31], the non-local signal R_{NL} can be written as

$$R_{NL} = \frac{V_{NL}}{I} = \pm \frac{1}{2} P^2 \frac{l_s}{\sigma A} e^{-dl/l_s} \quad (9)$$

I is the total current injected from $T2$; P is the spin polarization of $T2$ and $T3$ (that are identical because both of them are based on the CoFeB/MgO/Ge template); σ and A are the conductivity and the cross sectional area of the semiconductor channel, respectively. The factor $1/2$ is a consequence of the isotropic spin diffusion in the semiconductor. The $+$ ($-$) sign corresponds to the parallel (anti-parallel) orientation of $T2$ and $T3$ magnetizations. Note that equation (9) applies to a Ge channel, where the transport is forced to be planar and parallel to the Ge surface, while we are considering a Ge substrate, in which carriers can follow 3D pathways from $T2$ to $T3$. In the latter case, the mean pathway length is larger than in the former, because an additional dimension (the vertical one) is added. This reflects in a reduction of ΔR_{NL} , because the probability of suffering a spin-flip event moving from $T2$ to $T3$ increases. Anyway, assuming that the electrostatic configuration around $T2$ is independent on the $T2$ – $T3$ spacing d in our

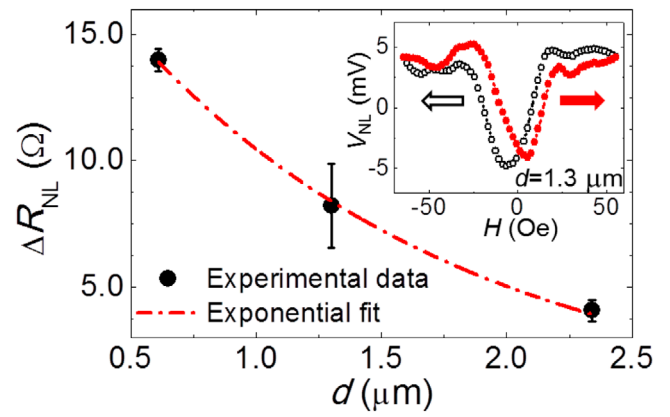


Figure 4. Non-local resistance measurement performed on the four-terminal structure shown in figure 3(b) [21]. From the fit of ΔR_{NL} versus d a spin diffusion length $l_s = 1.3 \pm 0.2$ μm at room temperature can be extracted. In the inset is reported the non-local voltage (V_{NL}), after subtraction of a small offset, as a function of the external field, showing two resistance levels corresponding to parallel (high resistance) and antiparallel (low resistance) configurations of the $T2$ and $T3$ magnetizations. Black (red) arrow indicates the sweeping direction of the field, from positive (negative) to negative (positive) values. Reproduced with permission from [21]. Copyright 2014 SPIE.

device (there is neither applied voltage nor applied current between $T2$ and $T3$), carriers diffuse from $T2$ to $T3$ independently on d , and thus the reduction of ΔR_{NL} with respect to the planar model should be roughly the same for all spacing.

All NL measurements were performed at RT by using a Keithley 6221 current source and a Keithley 2182A nanovoltmeter. In the inset of figure 4 we report V_{NL} as a function of the in-plane magnetic field H , after subtraction of a small voltage offset [32], for a spacing $d = 1.3$ μm between $T2$ and $T3$. The current I between $T1$ and $T2$ was 1 mA and the corresponding voltage drop was about 0.1 V. Note that, despite the low doping of Ge, no relevant Schottky barrier develops because of the depinning of the Fermi level at the Ge/MgO interface [18], so that transport at the terminals is dominated by tunnelling across the MgO barrier.

The shape of the ΔR_{NL} curve suggests that a fully antiparallel configuration of $T2$ and $T3$ magnetizations has not been achieved. This effect is present and essentially identical for all spacings (both the peak width and position are the same, independently on d). This means that, while the absolute value of ΔR_{NL} changes, the trend of ΔR_{NL} versus d does not. Because this effect, as well as the deviation from planar transport discussed above, globally do not affect the ΔR_{NL} versus d trend, the derivation of the spin diffusion length from the data trend in figure 4 can be considered correct.

Two resistance levels can be distinguished, due to the two possible orientations (parallel/antiparallel) of $T2$ and $T3$ magnetizations. The NL resistance value is lower (higher) for anti-parallel (parallel) relative orientation of $T2$ and $T3$ magnetizations. This is coherent with equation (9), predicting a positive (negative) R_{NL} in the case of parallel (anti-parallel) configuration. At large negative fields, the magnetizations of $T2$ and $T3$ are parallel, and R_{NL} is at maximum. As the field increases, $T3$ switches towards an antiparallel orientation with $T2$, and R_{NL} decreases until its minimum, that reaches at a field

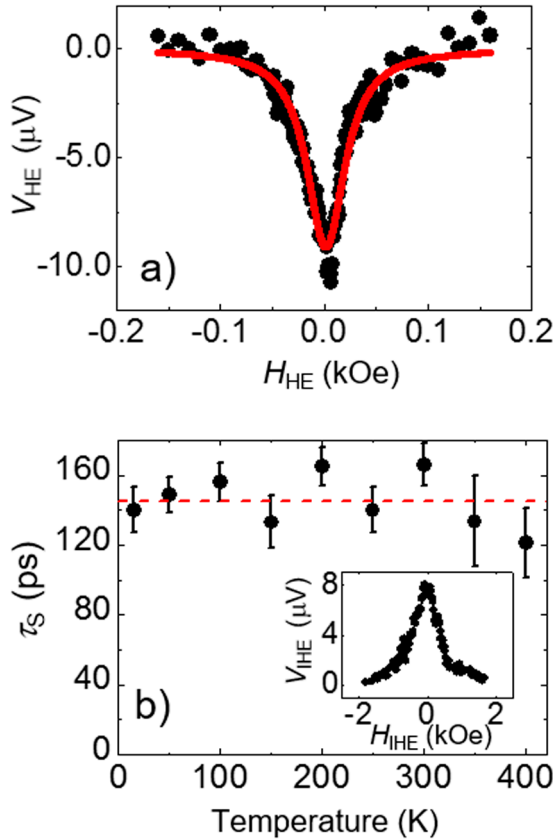


Figure 5. (a) Hanle effect measurement at room [21], giving a spin lifetime $\tau_s = 165 \pm 11 \text{ ps}$ obtained from the Lorentzian fit (red curve) of experimental data (black dots). (b) Spin lifetime versus temperature [21]. Spin lifetime is essentially temperature independent, with a mean value of 145 ps . In the inset is reported the inverted Hanle effect measurement at room temperature, suggesting the presence of residual interface roughness. Reproduced with permission from [21]. Copyright 2014 SPIE.

of 6 Oe. As the field increases further, $T2$ switches toward a parallel orientation of $T2$ and $T3$, and R_{NL} comes back to its maximum. The sequence is reversed when the magnetic field direction is swept from positive to negative. Following [25], that employs a $\text{Fe}/\text{Al}_2\text{O}_3/\text{Si}$ heterostructure for NL and AMR measurements in a lateral transport geometry, the width of the minima peaks suggests that the hysteresis loop of each terminal is not perfectly squared but elongated and rounded, due to edge inhomogeneities produced during the fabrication by EBL and/or domain wall formation and propagation in the ferromagnet.

In order to extrapolate the spin diffusion length (l_s) from NL measurements by equation (9), many devices with different spacing d (from $0.6 \mu\text{m}$ to $2.4 \mu\text{m}$) were fabricated. Figure 4 shows the difference between the NL resistances for parallel and anti-parallel alignment of the central electrodes (ΔR_{NL}), as a function of their distance (d). The use of ΔR_{NL} permits to remove the constant background contribution. ΔR_{NL} decreases with d because of spin-flip events occurring during the diffusion of carriers from the spin injector ($T2$) to the analyser ($T3$), reducing the splitting of the spin-dependent electrochemical potential at $T3$. According to equation (9), we fitted the experimental data by an exponential trend ($\Delta R_{NL} \approx e^{-d/l_s}$, red line in figure 4), obtaining a spin

diffusion length $l_s = 1.3 \pm 0.2 \mu\text{m}$ at room temperature. Using $l_s = \sqrt{D\tau_s}$ with $D = 0.01035 \text{ m}^2 \text{ s}^{-1}$ as above, the corresponding spin lifetime is $\tau_s \approx 160 \pm 60 \text{ ps}$.

4.2. Hanle and inverted Hanle effects

The experimental setup for the Hanle effect (HE) and inverted Hanle effect (IHE) is shown in figure 3(c). Only three terminals are required, with the central one acting both as a spin source and spin detector [23]. In HE, an external magnetic field (H_{HE}) is applied along the out-of-plane direction. Current flows between $T1'$ (reference terminal) and $T2'$, while the voltage is measured between $T2'$ (acting both as spin injector and detector) and $T3'$ (reference terminal). The spacing between adjacent terminals is about $100 \mu\text{m}$, much larger than the spin diffusion length. Spins injected from $T2'$ into the semiconductor lie in-plane as the magnetization of $T2'$. The external out-of-plane magnetic field causes a gyroscopic motion of carrier's spins around H_{HE} (Larmor precession) and the result is a spin dephasing that reduces the net spin polarization in the semiconductor as H_{HE} increases. The voltage difference between $T2'$ and $T3'$ (V_{HE}) is related to the difference between electrochemical potentials for the two in-plane spin components ($\Delta\mu = \mu^\uparrow - \mu^\downarrow$) underneath $T2'$ ($T3'$ has zero spin polarization underneath). The effect of H_{HE} is described by a Lorentzian line-shape [23]:

$$\Delta\mu(H_{HE}) = \frac{\Delta\mu(0)}{1 + (\omega_L\tau_s)^2} \quad (10)$$

where τ_s is the spin lifetime, $\omega_L = g\mu_B B_{HE}/\hbar$ is the Larmor frequency, g is the Landé g -factor, μ_B is the Bohr magneton and $B_{HE} = \mu_0 H_{HE}$ is the applied magnetic field. The relationship between $\Delta\mu$ and the measured voltage is $V_{HE} = \frac{\Delta\mu \cdot \gamma}{2e}$ [23], where γ is the tunnelling spin polarization of the CoFeB/MgO interface. From the fitting of V_{HE} versus H_{HE} using the Lorentzian lineshape of equation (10) and assuming $g = 1.6$ for Ge [33], the value of τ_s can be extracted.

The HE measurements were performed at different temperatures, from 15 K to 400 K , in a closed circuit He cryostat. A current of 2 mA was injected by $T2'$. Note that the Hanle effect was measured on the same sample used for NL measurements. In such a way, we were able to compare the NL and HE/IHE results on the very same structure, excluding any fabrication-related difference. In figure 5(a) we reported the HE voltage, after subtraction of a small offset, versus external field (V_{HE} versus H_{HE}) at 300 K , from which a spin lifetime $\tau_s = 165 \pm 11 \text{ ps}$ is obtained. Using $l_s = \sqrt{D\tau_s}$ with $D = 0.01035 \text{ m}^2 \text{ s}^{-1}$ as above, the corresponding spin diffusion length is $l_s \approx 1.3 \pm 0.08 \mu\text{m}$.

A rough surface or interface causes the presence of magnetic dipoles in the magnetic layer, and consequently the generation of random magnetostatic fields within the semiconductor, leading to an additional spurious spin dephasing term close to the interface [23]. Therefore, the spin lifetime τ_s measured by HE is usually underestimated because the precession along

Table 1. Spin diffusion length and lifetime at room temperature in intrinsic Ge obtained using the optical spin orientation, NL electrical measurements and Hanle effect.

Method	l_{sf} (μm)	τ_s (ps)
Optical orientation	0.9 ± 0.2	80 ± 40
Non-local electrical	1.3 ± 0.2	160 ± 60
Hanle effect	$\geq 1.3 \pm 0.08$	$\geq 165 \pm 11$

the local field is an additional source of depolarization⁷. In order to evaluate the presence of local magnetostatic fields, inverse Hanle effect (IHE) can be employed [24]. It is experimentally performed as the HE but with the external magnetic field (H_{IHE}) applied in the plane of the sample. The physical concept is the following: in case of zero external magnetic field H_{IHE} , injected spins precess around the axis determined by the random magnetostatic field, causing spin dephasing. If a strong enough in-plane magnetic field is present, roughness-related spurious magnetic moments in the magnetic layer are forced to align, so that the precession due their random distribution is removed and the spin signal is recovered.

In the inset of figure 5(b) is reported the IHE voltage versus external field (V_{IHE} versus H_{IHE}) at 300 K, in the same conditions of the HE above: the presence of a clear peak, of the same intensity of that measured by HE, suggests that random magnetic fields are present due to residual interface roughness. This effect, as well other contributions due to carrier scattering in the semiconductor and with barrier defects [35], definitely means that the values found above for τ_s and l_s must be assumed as lower bounds for the spin lifetime and spin diffusion length, respectively [24].

In figure 5(b) is reported the temperature dependence of τ_s , evaluated by Lorentzian fitting of the HE measurements at different temperatures. τ_s appears almost constant with only a small decrease above RT. Indeed, over the whole temperature range (15 K–400 K), the value of τ_s is between 120 and 160 ps, with a mean value of 145 ps. This behaviour is coherent with the observations of [34, 36], stating that the spin lifetime is limited by the spin precession induced by the surface roughness and spurious magnetic moments.

Table 1 summarizes the spin diffusion lengths and lifetimes at room temperature obtained employing the three methods described above, with the corresponding error bars. The two standard electrical methods (i.e. non-local electrical and Hanle effects) provide essentially the same result, while the optical orientation technique leads to a smaller value. This difference can be ascribed to two sources of uncertainty of which spin orientation suffers, with respect to the electrical techniques: (i) the degree of spin polarization versus photon energy ($P_S(h\nu)$) comes from theoretical calculations at 0K [25]); (ii) the dependence on $h\nu$ of the absorption length of Ge close to the band gap could affect the fit in this region [27]. In general, it is well known that different techniques can lead to partially different values, because it is difficult to extract the

bare semiconductor contribution. For example, in all-electrical measurements the spin flip contributions from scattering at the Fe/MgO and MgO/Ge interfaces, as well as the spin diffusion in the barrier, add up to spin flip events in Germanium to determine the total spin relaxation rate, while in all-optical measurements these spurious effects are absent. In this sense, all the spin diffusion lengths and times measured in a given experiment must be better intended as effective, instead that absolute.

However, the key point we want to underline in this paper is that all the three cited methods predict the same order of magnitude for the spin diffusion length (about 1 micron) and lifetime (about 100ps), coherently with [5], and this lifetime represents a lower limit due to the contribution of surface roughness and spurious magnetic moments to the spin de-phasing. The minor differences we noticed ($l_s = 0.9 \mu\text{m}$ from optical orientation versus $l_s = 1.3 \mu\text{m}$ from electrical methods), instead, are less relevant and can be regarded as a second-order effects related to the experimental configuration.

5. Conclusions

In this paper, we reported on the measurements of spin diffusion length and lifetime in Ge(001) by a novel method based on optical spin orientation with circularly polarized light. We confirm the results by comparison with measurements performed by more standard and validated electrical methods, based on electrical spin injection and detection in three- and four-terminal devices.

The two standard electrical methods provide essentially the same value of spin diffusion length at room temperature ($1.3 \pm 0.2 \mu\text{m}$ and $1.3 \pm 0.08 \mu\text{m}$ by NL and HE methods, respectively). Optical measurements at different photon energies, fitted by a model describing the energy dependence of the spin signal, give instead a smaller spin diffusion length at room temperature ($0.9 \pm 0.2 \mu\text{m}$), coherent with previous works and still compatible with the other methods. The small discrepancy could be related to the parameters of the material (the calculated degree of spin optical orientation and the light absorption length in the semiconductor versus the photon energy) and/or minor differences between the samples. Finally, we can conclude that the method we proposed, based on the electrical detection of optical orientation by spin-PDs, can be considered as a novel and reliable tool for the spin diffusion length and lifetime measurements for all the semiconductors with non-negligible degree of optical spin orientation (Ge, GaAs, CdSe...).

Acknowledgments

The authors thank M Leone for his skillful technical support and G Isella, F Pezzoli and A Giorgioni for fruitful discussions. This work was partially funded by Fondazione Cariplo, grants. no. 2013-0623 and 2013-0726, by EU FP7 Graphene Flagship (grant No. 604391), and by Ministero dell'Istruzione, dell'Università e della Ricerca through the project FIRB OSSIDI NANOSTRUTTURATI: MULTI-FUNZIONALITÀ E APPLICAZIONI (RBAP115AYN).

⁷Note that surface roughness does not play any role in spin-PDs: as a matter of fact, the Fe magnetization is saturated out-of-plane by an external magnetic field collinear to the photon angular momentum, so that magnetic moments are always oriented in such direction.

References

- [1] Awschalom D D, Loss D and Samarth N 2002 *Semiconductor Spintronics and Quantum Computation* (Berlin: Springer)
- [2] Giorgioni A, Vitiello E, Grilli E, Guzzi M and Pezzoli F 2014 *Appl. Phys. Lett.* **105** 152404
- [3] Loren E J, Ruzicka B A, Werake L K, Zhao H, van Driel H M and Smirl A L 2009 *Appl. Phys. Lett.* **95** 092107
- [4] Hanbicki A T, Cheng S-F, Goswami R, van't Erve O M J and Jonker B T 2012 *Solid State Commun.* **152** 244
- [5] Patibandla S, Atkinson G M, Bandyopadhyay S and Tepper G C 2010 *Physica E* **42** 1721
- [6] Guite C and Venkataraman V 2011 *Phys. Rev. Lett.* **107** 166603
- [7] Dushenko S, Koike M, Ando Y, Dhinjo T, Myronov M and Shiraishi M 2015 *Phys. Rev. Lett.* **114** 196602
- [8] Shen C et al 2010 *Appl. Phys. Lett.* **97** 162104
- [9] Ganichev S D et al 2007 *Phys. Rev. B* **75** 155317
- [10] Zhou Y, Han W, Chang L-T, Xiu F, Wang M, Oehme M, Fischer I A, Schulze J, Kawakami R K and Wang K L 2011 *Phys. Rev. B* **84** 125323
- [11] Rinaldi C, Cantoni M, Petti D, Sottocorno A, Leone M, Caffrey N M, Sanvito S and Bertacco R 2012 *Adv. Mater.* **24** 3037
- [12] Fert A and Jaffrès H 2001 *Phys. Rev. B* **64** 184420
- [13] Parkin S S, Kaiser C, Panchula A, Rice P M, Hughes B, Samant M and Yang S-H 2004 *Nat. Mater.* **3** 862
- [14] Han W, Zhou Y, Wang K L and Kawakami R K 2009 *J. Cryst. Growth* **312** 44
- [15] Jeon K-R, Park C-Y and Shin S-C 2010 *Cryst. Growth Des.* **10** 1346
- [16] Cantoni M, Petti D, Rinaldi C and Bertacco R 2011 *Microelectron. Eng.* **88** 530
- [17] Petti D, Cantoni M, Rinaldi C, Brivio S, Bertacco R, Gazquez J and Varela M 2011 *J. Appl. Phys.* **109** 084909
- [18] Cantoni M, Petti D, Rinaldi C and Bertacco R 2011 *Appl. Phys. Lett.* **98** 032104
- [19] Rinaldi C, Cantoni M, Petti D and Bertacco R 2012 *J. Appl. Phys.* **111** 07C312
- [20] Rinaldi C, Espahbodi M, Cantoni M and Bertacco R 2012 *Proc. SPIE* **8461** 84611F
- [21] Rinaldi C, Bertoli S, Cantoni M, Manzoni C, Cerullo G, Bianchi M, Sordan R and Bertacco R 2014 *Proc. SPIE* **9167** 916709
- [22] Bertacco R, Cantoni M, Riva M, Tagliaferri A and Ciccacci F 2005 *Appl. Surf. Sci.* **252** 1754
- [23] Dash S P, Sharma S, Patel R S, de Jong M P and Jansen R 2009 *Nature* **462** 491
- [24] Dash S P, Sharma S, Le Breton J C, Peiro J, Jaffrès H, George J-M, Lemaitre A and Jansen R 2011 *Phys. Rev. B* **84** 054410
- [25] Rioux J and Sipe E 2010 *Phys. Rev. B* **81** 155215
- [26] Rinaldi C, Cantoni M, Marangoni M, Manzoni C, Cerullo G and Bertacco R 2014 *Phys. Rev. B* **90** 161304
- [27] Dash W C and Newman R 1955 *Phys. Rev.* **99** 1151
- [28] Lu Y et al 2006 *Appl. Phys. Lett.* **89** 152106
- [29] Mak G and van Driel H M 1994 *Phys. Rev. B* **49** 16817
- [30] Lu Y, Altman R A, Marley A, Rishton S A, Trouilloud P L and Xiao G 1997 *Appl. Phys. Lett.* **70** 2610
- [31] Jedema F J, Costache V M, Heersche H B, Baselmans J J A and van Wees B J 2002 *Appl. Phys. Lett.* **81** 5162
- [32] Liu E-S, Nah J, Varahramyan K M and Tutuc E 2010 *Nanoletters* **10** 3297
- [33] van't Erve O M J, Hanbicki A T, Holub M, Li C H, Awo-Affouda C, Thompson P E and Jonker B T 2007 *Appl. Phys. Lett.* **91** 212109
- [34] Feher G, Wilson D K and Gere E A 1959 *Phys. Rev. Lett.* **3** 25
- [35] Chang L-T, Han W, Zhou Y, Tang J, Fischer I A, Oehme M, Schulze J, Kawakami R K and Wang K L 2013 *Semicond. Sci. Technol.* **28** 015018
- [36] Jain A et al 2011 *Appl. Phys. Lett.* **99** 162102